Measurement of the CP Asymmetry in $B^0 \to K^{*0}\mu^+\mu^-$ Decays

R. Aaij *et al.**
(LHCb Collaboration)

(Received 17 October 2012; published 17 January 2013)

A measurement of the CP asymmetry in $B^0 \to K^{*0}\mu^+\mu^-$ decays is presented, based on 1.0 fb^{-1} of pp collision data recorded by the LHCb experiment during 2011. The measurement is performed in six bins of invariant mass squared of the $\mu^+\mu^-$ pair, excluding the J/ψ and $\psi(2S)$ resonance regions. Production and detection asymmetries are removed using the $B^0 \to J/\psi K^{*0}$ decay as a control mode. The integrated CP asymmetry is found to be $-0.072 \pm 0.040(\text{stat}) \pm 0.005(\text{syst})$, consistent with the standard model.

DOI: 10.1103/PhysRevLett.110.031801 PACS numbers: 13.20.He, 11.30.Er, 12.15.Mm, 12.60.Jv

The decay $B^0 \to K^{*0}(\to K^+\pi^-)\mu^+\mu^-$ is a flavor changing neutral current process that proceeds via electroweak loop and box diagrams in the standard model (SM) [1]. The decay is highly suppressed in the SM and therefore physics beyond the SM such as supersymmetry [2] can contribute with a comparable amplitude via gluino or chargino loop diagrams. A number of observables are sensitive to such contributions, including the partial rate of the decay, the $\mu^+\mu^-$ forward-backward asymmetry ($A_{\rm FB}$), and the CP asymmetry ($\mathcal{A}_{CP}$). The CP asymmetry for $B^0 \to K^{*0}\mu^+\mu^-$ is defined as

$$\mathcal{A}_{CP} = \frac{\Gamma(\bar{B}^0 \to \bar{K}^{*0}\mu^+\mu^-) - \Gamma(B^0 \to K^{*0}\mu^+\mu^-)}{\Gamma(\bar{B}^0 \to \bar{K}^{*0}\mu^+\mu^-) + \Gamma(B^0 \to K^{*0}\mu^+\mu^-)}, \quad (1)$$

where Γ is the decay rate and the initial flavor of the B meson is tagged by the charge of the kaon from the K^* decay. The CP asymmetry is predicted to be of the order 10^{-3} in the SM [3,4] but is sensitive to physics beyond the SM that changes the operator basis by modifying the mixture of the vector and axial-vector components [5,6]. Some models that include new phenomena enhance the observed CP asymmetry up to ± 0.15 [7]. The theoretical prediction within a given model has a small error as the form factor uncertainties, which are the dominant theoretical errors for the decay rate, cancel in the ratio.

The CP asymmetry in $B^0 \to K^{*0}\mu^+\mu^-$ decays has previously been measured by the Belle [8] and *BABAR* [9] collaborations, with both results consistent with the SM. The LHCb collaboration has recently demonstrated its potential in this area with the most precise measurement of $A_{\rm FB}$ [10], and in this Letter, the measurement of the CP asymmetry by LHCb is presented.

The LHCb detector [11] is a single-arm forward spectrometer covering the pseudorapidity range $2 < \eta < 5$, designed for the study of particles containing b or c quarks. The detector includes a high precision tracking system consisting of a silicon-strip vertex detector surrounding the pp interaction region, a large-area silicon-strip detector located upstream of a dipole magnet with a bending power of about 4 Tm, and three stations of silicon-strip detectors and straw drift tubes placed downstream. The combined tracking system has a momentum resolution $\Delta p/p$ that varies from 0.4% at 5 GeV/c to 0.6% at 100 GeV/c and an impact parameter resolution of 20 μm for tracks with high transverse momentum ($p_{\rm T}$). Charged hadrons are identified using two ring-imaging Cherenkov detectors. Photon, electron, and hadron candidates are identified by a calorimeter system consisting of scintillating-pad and preshower detectors, an electromagnetic calorimeter, and a hadronic calorimeter. Muons are identified by a system composed of alternating layers of iron and multiwire proportional chambers. The trigger consists of a hardware stage, based on information from the calorimeter and muon systems, followed by a software stage that makes use of a full event reconstruction.

The simulated events used in this analysis are produced using the PYTHIA 6.4 generator [12], with a choice of parameters specifically configured for LHCb [13]. The EVTGEN package [14] describes the decay of the particles and the GEANT4 toolkit [15] simulates the detector response, implemented as described in Ref. [16]. QED radiative corrections are generated with the PHOTOS package [17].

The events used in the analysis are selected by a dedicated muon hardware trigger and then by one or more of a set of different muon and topological software triggers [18,19]. The hardware trigger requires the muons have $p_{\rm T}$ greater than 1.48 GeV/c, and the software trigger requires one of the final state particles to have both $p_{\rm T} >$ 0.8 GeV/c and impact parameter with respect to all pp interaction vertices $>$100 μm [19]. Triggered candidates are subject to the same two-stage selection as that used in Ref. [10]. The first stage is a cut-based selection, which includes requirements on the B^0 candidate's vertex fit χ^2, flight distance and invariant mass, and each track's impact

*Full author list given at the end of the article.

parameters with respect to any interaction vertex, p_T and polar angle. Background from misidentified kaon and pion tracks is removed using information from the particle identification (PID) system, and muon tracks are required to have hits in the muon system. Finally, the production vertex of the B^0 candidate must lie within 5 mm of the beam axis in the transverse directions, and within 200 mm of the average interaction position in the beam (z) direction.

In the second stage, the candidates must pass a multivariate selection that uses a boosted decision tree [20] that implements the AdaBoost algorithm [21]. This is a tighter selection that takes into account other variables including the decay time and flight direction of the B^0 candidates, the p_T of the hadrons, measures of the track and vertex quality, and PID information for the daughter tracks. For the rest of the Letter, the inclusion of charge conjugate modes is implied unless explicitly stated.

In order to obtain a clean sample of $B^0 \to K^{*0}\mu^+\mu^-$ decays, the $c\bar{c}$ resonant decays $B^0 \to J/\psi K^{*0}$ and $B^0 \to \psi(2S)K^{*0}$ are removed by excluding events with $\mu^+\mu^-$ invariant mass, $m_{\mu^+\mu^-}$, satisfying $2.95 < m_{\mu^+\mu^-} < 3.18\,\mathrm{GeV}/c^2$ or $3.59 < m_{\mu^+\mu^-} < 3.77\,\mathrm{GeV}/c^2$. If $m_{K^+\pi^-\mu^+\mu^-} < 5.23\,\mathrm{GeV}/c^2$, then the vetoes are extended downwards by 0.15 GeV$/c^2$ to remove the radiative tails of the resonances. Backgrounds involving misidentified particles are vetoed using cuts on the masses of the B^0 and K^{*0} mesons and the $\mu^+\mu^-$ pair, as well as using the PID information for the daughter particles. These include $B_s^0 \to \phi\mu^+\mu^-$ candidates in which a kaon has been misidentified as a pion, $B^0 \to J/\psi K^{*0}$ candidates where a hadron is swapped with a muon, and $B^+ \to K^+\mu^+\mu^-$ candidates that combine with a random low momentum pion. The vetoes are described fully in Ref. [10]. $\mathcal{A}_{CP}$ may be diluted by $B^0 \to K^{*0}\mu^+\mu^-$ candidates with the kaon and pion misidentified as each other, which is estimated as 0.8% of the $B^0 \to K^{*0}\mu^+\mu^-$ yield using simulated events. All B^0 candidates must have a mass in the range 5.15–5.80 GeV$/c^2$; the tight low mass edge of this window serves to remove background from partially reconstructed B meson decays. All K^{*0} candidates must have an invariant mass of the kaon-pion pair within 0.1 GeV$/c^2$ of the nominal $K^{*0}(892)$ mass. A proton veto, using PID information from a neural network, is also applied to remove background from Λ_b decays, where a proton in the final state is misidentified as a kaon or pion in the $B^0 \to K^{*0}\mu^+\mu^-$ decay.

Approximately 2% of selected events contain two $B^0 \to K^{*0}\mu^+\mu^-$ candidates that have tracks in common. The majority of these candidates arise from swapping the assignment of the kaon and pion hypothesis. As the charges of the kaon and pion tag the flavor of the B meson these duplicate candidates can bias the measured value of $\mathcal{A}_{CP}$. This is accounted for by randomly removing one of the two candidates from the sample. This process is repeated many times over the full sample with a different random seed in each case and the average measured value of $\mathcal{A}_{CP}$ is taken as the result.

An accurate measurement of $\mathcal{A}_{CP}$ requires that the differences in the production rates (R) of $B^0/\bar{B}^0$ mesons and detection efficiencies (ϵ) between the $B^0 \to K^{*0}\mu^+\mu^-$ and $\bar{B}^0 \to \bar{K}^{*0}\mu^+\mu^-$ modes be accounted for. Assuming all asymmetries are small, the raw measured asymmetry may be expressed as

$$\mathcal{A}_{\mathrm{RAW}} = \mathcal{A}_{CP} + \kappa\mathcal{A}_P + \mathcal{A}_D, \tag{2}$$

where the production asymmetry, which is of the order of 1% [22], is defined as $\mathcal{A}_P \equiv [R(\bar{B}^0) - R(B^0)]/[R(\bar{B}^0) + R(B^0)]$ and the detection asymmetry is $\mathcal{A}_D \equiv [\epsilon(\bar{B}^0) - \epsilon(B^0)]/[\epsilon(\bar{B}^0) + \epsilon(B^0)]$. The production asymmetry is diluted through B^0-$\bar{B}^0$ oscillations by a factor κ

$$\kappa \equiv \frac{\int_0^\infty \epsilon(t)e^{-\Gamma t}\cos\Delta m t dt}{\int_0^\infty \epsilon(t)e^{-\Gamma t}dt}, \tag{3}$$

where t, Γ, and Δm are the decay time, mean decay rate, and mass difference between the light and heavy eigenstates of the B^0 meson, respectively. The quantity $\mathcal{A}_D$ is dominated by the $K^+\pi^-/K^-\pi^+$ detection asymmetry that arises due to left-right asymmetries in the LHCb detector and different interactions of positively and negatively charged tracks with the detector material. The left-right asymmetry is canceled by taking an average with equal weights of the CP asymmetries measured in two independent data samples with opposite polarities of the LHCb dipole magnet. These data samples correspond to 61% and 39% of the total data sample.

The production and interaction asymmetries are corrected for using the $B^0 \to J/\psi K^{*0}$ decay mode as a control channel. Since $B^0 \to K^{*0}\mu^+\mu^-$ and $B^0 \to J/\psi K^{*0}$ decays have the same final state and similar kinematics, the measured raw asymmetry for $B \to J/\psi K^{*0}$ decays may be simply expressed as $\mathcal{A}_{\mathrm{RAW}}(B^0 \to J/\psi K^{*0}) = \kappa\mathcal{A}_P + \mathcal{A}_D$, in the absence of a CP asymmetry. $B^0 \to J/\psi K^{*0}$ proceeds via a $b \to c\bar{c}s$ transition, as does the decay mode $B^+ \to J/\psi K^+$, and hence should have a CP asymmetry similar to $\mathcal{A}_{CP}(B^+ \to J/\psi K^+) = (1 \pm 7) \times 10^{-3}$ [23,24]. For this analysis, it is assumed that $\mathcal{A}_{CP}(B^0 \to J/\psi K^{*0}) = 0$. The CP asymmetry in $B^0 \to K^{*0}\mu^+\mu^-$ decays is then calculated as

$$\mathcal{A}_{CP} = \mathcal{A}_{\mathrm{RAW}}(B^0 \to K^{*0}\mu^+\mu^-) - \mathcal{A}_{\mathrm{RAW}}(B^0 \to J/\psi K^{*0}). \tag{4}$$

Noncanceling asymmetries due to differences between the kinematics of $B^0 \to K^{*0}\mu^+\mu^-$ and $B^0 \to J/\psi K^{*0}$ decays are considered systematic effects.

The full data sample, containing approximately 900 $B^0 \to K^{*0}\mu^+\mu^-$ signal decays, is split into the six bins of $\mu^+\mu^-$ invariant mass squared (q^2) used by the LHCb, Belle, and CDF angular analyses [8,10,25]. An additional bin of $1 < q^2 < 6$ GeV$^2/c^4$ is used, to be compared to the

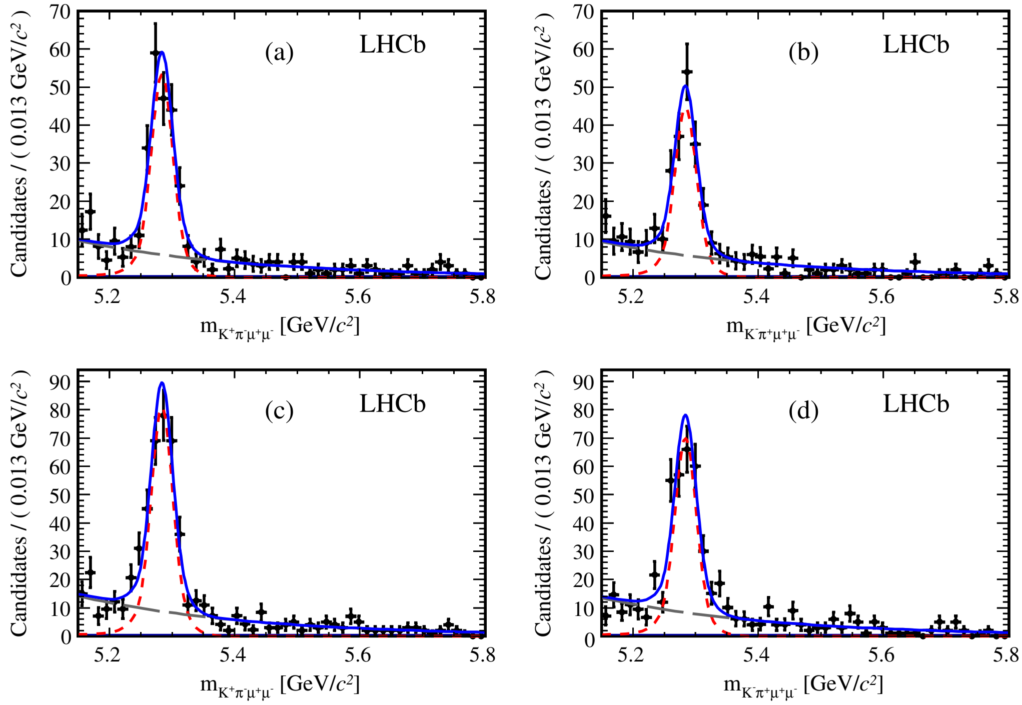

FIG. 1 (color online). Mass fits for $B^0 \to K^{*0}\mu^+\mu^-$ decays used to extract the integrated CP asymmetry. The curves displayed are the full mass fit (blue, solid line), the signal peak (red, short-dashed line), and the background (grey, long-dashed line). The mass fits on the top row correspond to the (a) B^0 and (b) $\bar{B}^0$ decays for one magnet polarity, while the bottom row shows the mass fits for (c) B^0 and (d) $\bar{B}^0$ for the reverse polarity.

theoretical prediction in Ref. [4]. The $B^0 \to J/\psi K^{*0}$ data sample contains approximately 104 000 signal decays with $3.04 < q^2 < 3.16\ \mathrm{GeV}^2/c^4$. The values of $\mathcal{A}_{CP}$ are measured using a simultaneous unbinned maximum-likelihood fit to the $B^0 \to K^{*0}\mu^+\mu^-$ and $B^0 \to J/\psi K^{*0}$ invariant mass distributions in the range 5.15–5.80 GeV/c^2. The simultaneous fit in each q^2 bin spans eight data samples, split between the initial particles B^0 and $\bar{B}^0$, the decay modes $B^0 \to K^{*0}\mu^+\mu^-$ and $B^0 \to J/\psi K^{*0}$, and magnet polarity, where the $B^0 \to J/\psi K^{*0}$ sample is common to all q^2 bins. This fit returns two values of $\mathcal{A}_{CP}$, one for each magnet polarity, and an average with equal weights is made to find the value of $\mathcal{A}_{CP}$ in that q^2 bin. An integrated value of $\mathcal{A}_{CP}$ over all q^2 is also calculated.

The signal invariant mass distributions for the $B^0 \to K^{*0}\mu^+\mu^-$ and $B^0 \to J/\psi K^{*0}$ decays are modeled using the sum of two Crystal Ball functions [26] with common peak and tail parameters but different widths. The values of the tail parameters are determined from fits to simulated events and fixed in the fit. Combinatorial background arising from the random misassociation of tracks to form a B^0 candidate is modeled using an exponential function. The $B^0 \to J/\psi K^{*0}$ fit also accounts for a peaking $B_s^0 \to J/\psi \bar{K}^{*0}$ contribution, which has the same shape as the signal and an expected yield that is $(0.7 \pm 0.2)\%$ of that of $B^0 \to J/\psi K^{*0}$ [27]. In the simultaneous fit, the signal shape is the same for the two modes, but the signal and background yields and the exponential background

TABLE I. Systematic uncertainties on $\mathcal{A}_{CP}$, from residual kinematic asymmetries, muon asymmetry, choice of signal model, and the modeling of the mass resolution, for each q^2 bin. The total uncertainty is calculated by adding the individual uncertainties in quadrature.

	Sources of systematic uncertainties					
q^2 region (GeV^2/c^4)	Multiple cands.	Residual asymmetries	$\mu^\pm$ detection asymmetry	Signal model	Mass resol.	Total
$0.05 < q^2 < 2.00$	0.002	0.007	0.005	0.005	0.001	0.010
$2.00 < q^2 < 4.30$	0.006	0.007	0.006	0.007	0.010	0.016
$4.30 < q^2 < 8.68$	0.004	0.003	0.006	0.004	0.003	0.010
$10.09 < q^2 < 12.86$	0.003	0.007	0.009	0.001	0.002	0.011
$14.18 < q^2 < 16.00$	0.001	0.006	0.007	0.001	0.001	0.009
$16.00 < q^2 < 20.00$	0.003	0.005	0.003	0.003	0.009	0.012
$1.00 < q^2 < 6.00$	0.001	0.006	0.005	0.002	0.003	0.009
$0.05 < q^2 < 20.00$	0.002	0.002	0.005	0.001	0.001	0.005

TABLE II. Values of $\mathcal{A}_{CP}$ for $B^0 \to K^{*0}\mu^+\mu^-$ in the q^2 bins used in the analysis.

q^2 region (GeV$^2/c^4$)	Signal yield	$\mathcal{A}_{CP}$	Statistical uncertainty	Systematic uncertainty	Total uncertainty
$0.05 < q^2 < 2.00$	168 ± 15	-0.196	0.094	0.010	0.095
$2.00 < q^2 < 4.30$	72 ± 11	-0.098	0.153	0.016	0.154
$4.30 < q^2 < 8.68$	266 ± 19	-0.021	0.073	0.010	0.075
$10.09 < q^2 < 12.86$	157 ± 15	-0.054	0.097	0.011	0.098
$14.18 < q^2 < 16.00$	116 ± 12	-0.201	0.104	0.009	0.104
$16.00 < q^2 < 20.00$	128 ± 13	0.089	0.100	0.012	0.101
$1.00 < q^2 < 6.00$	194 ± 17	-0.058	0.064	0.009	0.064
$0.05 < q^2 < 20.00$	904 ± 35	-0.072	0.040	0.005	0.040

parameter may vary. Figure 1 shows the mass fit to the $B^0 \to K^{*0}\mu^+\mu^-$ decay in the full q^2 range.

Many sources of systematic uncertainty cancel in the difference of the raw asymmetries between $B^0 \to K^{*0}\mu^+\mu^-$ and $B^0 \to J/\psi K^{*0}$ decays and in the average of CP asymmetries measured using data recorded with opposite magnet polarities. However, systematic uncertainties can arise from residual noncanceling asymmetries due to the different kinematic behavior of $B^0 \to K^{*0}\mu^+\mu^-$ and $B^0 \to J/\psi K^{*0}$ decays. The effect is estimated by reweighting $B^0 \to J/\psi K^{*0}$ candidates so that their kinematic variables are distributed in the same way as for $B^0 \to K^{*0}\mu^+\mu^-$ candidates. The value of $\mathcal{A}_{\rm RAW}(B^0 \to J/\psi K^{*0})$ is then calculated for these reweighted events and the difference from the default value is taken as the systematic uncertainty. This procedure is carried out separately for a number of quantities including the p, $p_{\rm T}$, and pseudorapidity of the B^0 and the K^{*0} mesons. The total systematic uncertainty associated with the different kinematic behavior of the two decays is calculated by adding each individual contribution in quadrature. This is conservative, as many of the variables are correlated.

The random removal of multiple candidates discussed above also introduces a systematic uncertainty on $\mathcal{A}_{CP}$. The uncertainty on the mean value of $\mathcal{A}_{CP}$ from the ten different random removals is taken as the systematic uncertainty.

The forward-backward asymmetry in $B^0 \to K^{*0}\mu^+\mu^-$ decays [10], which varies as a function of q^2, causes positive and negative muons to have different momentum distributions. Different detection efficiencies for positive and negative muons introduce an asymmetry that cannot be accounted for by the $B^0 \to J/\psi K^{*0}$ decay, which does not have a comparable forward-backward asymmetry. The selection efficiencies for positive and negative muons are evaluated using muons from J/ψ decay in data and the resulting asymmetry in the selected $B^0 \to K^{*0}\mu^+\mu^-$ sample is calculated in each q^2 bin.

A number of possible effects due to the choice of model for the mass fit are considered. The signal model is replaced with a sum of two Gaussian distributions and a possible difference in the mass resolution for $B^0 \to K^{*0}\mu^+\mu^-$ and $B^0 \to J/\psi K^{*0}$ decays is investigated by allowing the width of the $B^0 \to K^{*0}\mu^+\mu^-$ signal peak to vary in a range of 0.7–1.3 times that of the $B^0 \to J/\psi K^{*0}$ model. These systematic uncertainties are summarized in Table I. As a further cross-check, $\mathcal{A}_{CP}$ is calculated using a weighted average of the measurements from the six q^2 bins and the result is found to be consistent with that obtained from the integrated data set.

The results of the full $\mathcal{A}_{CP}$ fit are presented in Table II and Fig. 2. The raw asymmetry in $B^0 \to J/\psi K^{*0}$ decays is measured as

$$\mathcal{A}_{\rm RAW}(B^0 \to J/\psi K^{*0}) = -0.0110 \pm 0.0032 \pm 0.0006,$$

where the first uncertainty is statistical and the second is systematic. The CP asymmetry integrated over the full q^2 range is calculated and found to be

$$\mathcal{A}_{CP}(B^0 \to K^{*0}\mu^+\mu^-) = -0.072 \pm 0.040 \pm 0.005.$$

The result is consistent with previous measurements made by Belle [8], $\mathcal{A}_{CP}$ $(B \to K^* l^+ l^-) = -0.10 \pm 0.10 \pm 0.01$, and *BABAR* [9], $\mathcal{A}_{CP}$ $(B \to K^* l^+ l^-) = 0.03 \pm 0.13 \pm 0.01$. This measurement is significantly more

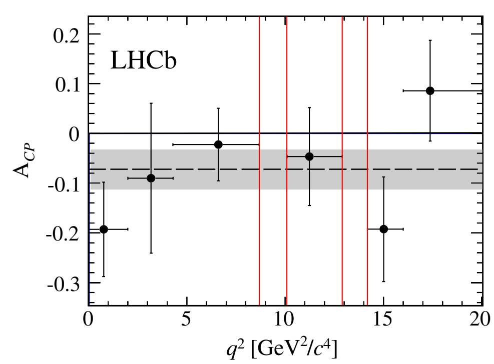

FIG. 2 (color online). Fitted value of $\mathcal{A}_{CP}$ in $B^0 \to K^{*0}\mu^+\mu^-$ decays in bins of the $\mu^+\mu^-$ invariant mass squared (q^2). The red vertical lines mark the charmonium vetoes. The points are plotted at the mean value of q^2 in each bin. The uncertainties on each $\mathcal{A}_{CP}$ value are the statistical and systematic uncertainties added in quadrature. The dashed line corresponds to the q^2 integrated value, and the grey band is the 1σ uncertainty on this value.

precise than all other measurements of $\mathcal{A}_{CP}$ in $B^0 \to K^{*0}\mu^+\mu^-$ decays to date.

We express our gratitude to our colleagues in the CERN accelerator departments for the excellent performance of the LHC. We thank the technical and administrative staff at the LHCb institutes. We acknowledge support from CERN and from the national agencies: CAPES, CNPq, FAPERJ, and FINEP (Brazil); NSFC (China); CNRS/IN2P3 and Region Auvergne (France); BMBF, DFG, HGF, and MPG (Germany); SFI (Ireland); INFN (Italy); FOM and NWO (The Netherlands); SCSR (Poland); ANCS/IFA (Romania); MinES, Rosatom, RFBR, and NRC "Kurchatov Institute" (Russia); MinECo, XuntaGal, and GENCAT (Spain); SNSF and SER (Switzerland); NAS Ukraine (Ukraine); STFC (United Kingdom); NSF (USA). We also acknowledge support received from the ERC under FP7. The Tier1 computing centers are supported by IN2P3 (France), KIT, and BMBF (Germany), INFN (Italy), NWO and SURF (The Netherlands), CIEMAT, IFAE, and UAB (Spain), and GridPP (United Kingdom). We are thankful for the computing resources put at our disposal by Yandex LLC (Russia), as well as to the communities behind the multiple open source software packages that we depend on.

[1] F. Kruger, L. M. Sehgal, N. Sinha, and R. Sinha, Phys. Rev. D **61**, 114028 (2000).
[2] P. Fayet and S. Ferrara, Phys. Rep. **32**, 249 (1977).
[3] C. Bobeth, G. Hiller, and G. Piranishvili, J. High Energy Phys. 07 (2008) 106.
[4] W. Altmannshofer, P. Ball, A. Bharucha, A. J Buras, D. M. Straub, and M. Wick, J. High Energy Phys. 01 (2009) 019.
[5] A. Ali and G. Hiller, Eur. Phys. J. C **8**, 619 (1999).
[6] C. Bobeth, G. Hiller, D. van Dyk, and C. Wacker, J. High Energy Phys. 01 (2012) 107.
[7] A. K. Alok, A. Datta, A. Dighe, M. Duraisamy, D. Ghosh, and D. London, J. High Energy Phys. 11 (2011) 122.
[8] J.-T. Wei *et al.* (Belle Collaboration), Phys. Rev. Lett. **103**, 171801 (2009).
[9] J. Lees *et al.* (*BABAR* Collaboration), Phys. Rev. D **86**, 032012 (2012).
[10] R. Aaij *et al.* (LHCb Collaboration), Phys. Rev. Lett. **108**, 181806 (2012); R. Aaij *et al.*, Report No. LHCb-CONF-2012-008.
[11] A. A. Alves, Jr. *et al.* (LHCb Collaboration), JINST **3**, S08005 (2008).
[12] T. Sjöstrand, S. Mrenna, and P. Skands, J. High Energy Phys. 05 (2006) 026.
[13] I. Belyaev *et al.*, *Nuclear Science Symposium Conference Record (NSS/MIC)* (IEEE, New York, 2010), p. 1155.
[14] D. J. Lange, Nucl. Instrum. Methods Phys. Res., Sect. A **462**, 152 (2001).
[15] J. Allison *et al.* (GEANT4 Collaboration), IEEE Trans. Nucl. Sci. **53**, 270 (2006); S. Agostinelli *et al.* (GEANT4 Collaboration), Nucl. Instrum. Methods Phys. Res., Sect. A **506**, 250 (2003).
[16] M. Clemencic, G. Corti, S. Easo, C. R. Jones, S. Miglioranzi, M. Pappagallo, and P. Robbe, J. Phys. Conf. Ser. **331**, 032023 (2011).
[17] P. Golonka and Z. Was, Eur. Phys. J. C **45**, 97 (2006).
[18] R. Aaij and J. Albrecht, Report No. LHCb-PUB-2011-017.
[19] V. V. Gligorov, C. Thomas, and M. Williams, Report No. LHCb-PUB-2011-016.
[20] L. Breiman, J. H. Friedman, R. A. Olshen, and C. J. Stone, *Classification and Regression Trees* (Wadsworth International Group, Belmont, California 1984).
[21] R. E. Schapire and Y. Freund, J. Comput. Syst. Sci. **55**, 119 (1997).
[22] R. Aaij *et al.* (LHCb Collaboration), Phys. Rev. Lett. **108**, 201601 (2012).
[23] J. Beringer *et al.* (Particle Data Group), Phys. Rev. D **86**, 010001 (2012).
[24] V. Abazov *et al.* (D0 Collaboration), Phys. Rev. Lett. **100**, 211802 (2008).
[25] T. Aaltonen *et al.* (CDF Collaboration), Phys. Rev. Lett. **108**, 081807 (2012).
[26] T. Skwarnicki, PhD thesis, Krakow Institute of Nuclear Physics [Report No. DESY-F31-86-02, Krakow, 1986].
[27] R. Aaij *et al.* (LHCb Collaboration), Phys. Rev. D **86**, 071102(R) (2012).

R. Aaij,[38] C. Abellan Beteta,[33,n] A. Adametz,[11] B. Adeva,[34] M. Adinolfi,[43] C. Adrover,[6] A. Affolder,[49] Z. Ajaltouni,[5] J. Albrecht,[35] F. Alessio,[35] M. Alexander,[48] S. Ali,[38] G. Alkhazov,[27] P. Alvarez Cartelle,[34] A. A. Alves, Jr.,[22] S. Amato,[2] Y. Amhis,[36] L. Anderlini,[17,f] J. Anderson,[37] R. B. Appleby,[51] O. Aquines Gutierrez,[10] F. Archilli,[18,35] A. Artamonov,[32] M. Artuso,[53] E. Aslanides,[6] G. Auriemma,[22,m] S. Bachmann,[11] J. J. Back,[45] C. Baesso,[54] V. Balagura,[36,28] W. Baldini,[16] R. J. Barlow,[51] C. Barschel,[35] S. Barsuk,[7] W. Barter,[44] A. Bates,[48] Th. Bauer,[38] A. Bay,[36] J. Beddow,[48] I. Bediaga,[1] S. Belogurov,[28] K. Belous,[32] I. Belyaev,[28] E. Ben-Haim,[8] M. Benayoun,[8] G. Bencivenni,[18] S. Benson,[47] J. Benton,[43] A. Berezhnoy,[29] R. Bernet,[37] M.-O. Bettler,[44] M. van Beuzekom,[38] A. Bien,[11] S. Bifani,[12] T. Bird,[51] A. Bizzeti,[17,h] P. M. Bjørnstad,[51] T. Blake,[35] F. Blanc,[36] C. Blanks,[50] J. Blouw,[11] S. Blusk,[53] A. Bobrov,[31] V. Bocci,[22] A. Bondar,[31] N. Bondar,[27] W. Bonivento,[15] S. Borghi,[48,51] A. Borgia,[53] T. J. V. Bowcock,[49] C. Bozzi,[16] T. Brambach,[9] J. van den Brand,[39] J. Bressieux,[36] D. Brett,[51] M. Britsch,[10] T. Britton,[53] N. H. Brook,[43] H. Brown,[49] A. Büchler-Germann,[37] I. Burducea,[26] A. Bursche,[37] J. Buytaert,[35] S. Cadeddu,[15] O. Callot,[7] M. Calvi,[20,j] M. Calvo Gomez,[33,n] A. Camboni,[33] P. Campana,[18,35] A. Carbone,[14,c] G. Carboni,[21,k] R. Cardinale,[19,i] A. Cardini,[15] L. Carson,[50] K. Carvalho Akiba,[2] G. Casse,[49] M. Cattaneo,[35] Ch. Cauet,[9] M. Charles,[52] Ph. Charpentier,[35] P. Chen,[3,36] N. Chiapolini,[37] M. Chrzaszcz,[23] K. Ciba,[35] X. Cid Vidal,[34]

G. Ciezarek,[50] P. E. L. Clarke,[47] M. Clemencic,[35] H. V. Cliff,[44] J. Closier,[35] C. Coca,[26] V. Coco,[38] J. Cogan,[6] E. Cogneras,[5] P. Collins,[35] A. Comerma-Montells,[33] A. Contu,[52,15] A. Cook,[43] M. Coombes,[43] G. Corti,[35] B. Couturier,[35] G. A. Cowan,[36] D. Craik,[45] S. Cunliffe,[50] R. Currie,[47] C. D'Ambrosio,[35] P. David,[8] P. N. Y. David,[38] I. De Bonis,[4] K. De Bruyn,[38] S. De Capua,[21,k] M. De Cian,[37] J. M. De Miranda,[1] L. De Paula,[2] P. De Simone,[18] D. Decamp,[4] M. Deckenhoff,[9] H. Degaudenzi,[36,35] L. Del Buono,[8] C. Deplano,[15] D. Derkach,[14] O. Deschamps,[5] F. Dettori,[39] J. Dickens,[44] H. Dijkstra,[35] P. Diniz Batista,[1] F. Domingo Bonal,[33,n] S. Donleavy,[49] F. Dordei,[11] A. Dosil Suárez,[34] D. Dossett,[45] A. Dovbnya,[40] F. Dupertuis,[36] R. Dzhelyadin,[32] A. Dziurda,[23] A. Dzyuba,[27] S. Easo,[46] U. Egede,[50] V. Egorychev,[28] S. Eidelman,[31] D. van Eijk,[38] F. Eisele,[11] S. Eisenhardt,[47] R. Ekelhof,[9] L. Eklund,[48] I. El Rifai,[5] Ch. Elsasser,[37] D. Elsby,[42] D. Esperante Pereira,[34] A. Falabella,[14,c] C. Färber,[11] G. Fardell,[47] C. Farinelli,[38] S. Farry,[12] V. Fave,[36] V. Fernandez Albor,[34] F. Ferreira Rodrigues,[1] M. Ferro-Luzzi,[35] S. Filippov,[30] C. Fitzpatrick,[35] M. Fontana,[10] F. Fontanelli,[19,i] R. Forty,[35] O. Francisco,[2] M. Frank,[35] C. Frei,[35] M. Frosini,[17,f] S. Furcas,[20] A. Gallas Torreira,[34] D. Galli,[14,c] M. Gandelman,[2] P. Gandini,[52] Y. Gao,[3] J-C. Garnier,[35] J. Garofoli,[53] J. Garra Tico,[44] L. Garrido,[33] C. Gaspar,[35] R. Gauld,[52] E. Gersabeck,[11] M. Gersabeck,[35] T. Gershon,[45,35] Ph. Ghez,[4] V. Gibson,[44] V. V. Gligorov,[35] C. Göbel,[54] D. Golubkov,[28] A. Golutvin,[50,28,35] A. Gomes,[2] H. Gordon,[52] M. Grabalosa Gándara,[33] R. Graciani Diaz,[33] L. A. Granado Cardoso,[35] E. Graugés,[33] G. Graziani,[17] A. Grecu,[26] E. Greening,[52] S. Gregson,[44] O. Grünberg,[55] B. Gui,[53] E. Gushchin,[30] Yu. Guz,[32] T. Gys,[35] C. Hadjivasiliou,[53] G. Haefeli,[36] C. Haen,[35] S. C. Haines,[44] S. Hall,[50] T. Hampson,[43] S. Hansmann-Menzemer,[11] N. Harnew,[52] S. T. Harnew,[43] J. Harrison,[51] P. F. Harrison,[45] T. Hartmann,[55] J. He,[7] V. Heijne,[38] K. Hennessy,[49] P. Henrard,[5] J. A. Hernando Morata,[34] E. van Herwijnen,[35] E. Hicks,[49] D. Hill,[52] M. Hoballah,[5] P. Hopchev,[4] W. Hulsbergen,[38] P. Hunt,[52] T. Huse,[49] N. Hussain,[52] R. S. Huston,[12] D. Hutchcroft,[49] D. Hynds,[48] V. Iakovenko,[41] P. Ilten,[12] J. Imong,[43] R. Jacobsson,[35] A. Jaeger,[11] M. Jahjah Hussein,[5] E. Jans,[38] F. Jansen,[38] P. Jaton,[36] B. Jean-Marie,[7] F. Jing,[3] M. John,[52] D. Johnson,[52] C. R. Jones,[44] B. Jost,[35] M. Kaballo,[9] S. Kandybei,[40] M. Karacson,[35] M. Karbach,[35] J. Keaveney,[12] I. R. Kenyon,[42] U. Kerzel,[35] T. Ketel,[39] A. Keune,[36] B. Khanji,[20] Y. M. Kim,[47] O. Kochebina,[7] I. Komarov,[29] V. Komarov,[36] R. F. Koopman,[39] P. Koppenburg,[38] M. Korolev,[29] A. Kozlinskiy,[38] L. Kravchuk,[30] K. Kreplin,[11] M. Kreps,[45] G. Krocker,[11] P. Krokovny,[31] F. Kruse,[9] M. Kucharczyk,[20,23,j] V. Kudryavtsev,[31] T. Kvaratskheliya,[28,35] V. N. La Thi,[36] D. Lacarrere,[35] G. Lafferty,[51] A. Lai,[15] D. Lambert,[47] R. W. Lambert,[39] E. Lanciotti,[35] G. Lanfranchi,[18,35] C. Langenbruch,[35] T. Latham,[45] C. Lazzeroni,[42] R. Le Gac,[6] J. van Leerdam,[38] J.-P. Lees,[4] R. Lefèvre,[5] A. Leflat,[29,35] J. Lefrançois,[7] O. Leroy,[6] T. Lesiak,[23] L. Li,[3] Y. Li,[3] L. Li Gioi,[5] M. Liles,[49] R. Lindner,[35] C. Linn,[11] B. Liu,[3] G. Liu,[35] J. von Loeben,[20] J. H. Lopes,[2] E. Lopez Asamar,[33] N. Lopez-March,[36] H. Lu,[3] J. Luisier,[36] A. Mac Raighne,[48] F. Machefert,[7] I. V. Machikhiliyan,[4,28] F. Maciuc,[26] O. Maev,[27,35] J. Magnin,[1] M. Maino,[20] S. Malde,[52] G. Manca,[15,d] G. Mancinelli,[6] N. Mangiafave,[44] U. Marconi,[14] R. Märki,[36] J. Marks,[11] G. Martellotti,[22] A. Martens,[8] L. Martin,[52] A. Martín Sánchez,[7] M. Martinelli,[38] D. Martinez Santos,[35] A. Massafferri,[1] Z. Mathe,[35] C. Matteuzzi,[20] M. Matveev,[27] E. Maurice,[6] A. Mazurov,[16,30,35] J. McCarthy,[42] G. McGregor,[51] R. McNulty,[12] M. Meissner,[11] M. Merk,[38] J. Merkel,[9] D. A. Milanes,[13] M.-N. Minard,[4] J. Molina Rodriguez,[54] S. Monteil,[5] D. Moran,[51] P. Morawski,[23] R. Mountain,[53] I. Mous,[38] F. Muheim,[47] K. Müller,[37] R. Muresan,[26] B. Muryn,[24] B. Muster,[36] J. Mylroie-Smith,[49] P. Naik,[43] T. Nakada,[36] R. Nandakumar,[46] I. Nasteva,[1] M. Needham,[47] N. Neufeld,[35] A. D. Nguyen,[36] C. Nguyen-Mau,[36,o] M. Nicol,[7] V. Niess,[5] N. Nikitin,[29] T. Nikodem,[11] A. Nomerotski,[52,35] A. Novoselov,[32] A. Oblakowska-Mucha,[24] V. Obraztsov,[32] S. Oggero,[38] S. Ogilvy,[48] O. Okhrimenko,[41] R. Oldeman,[15,35,d] M. Orlandea,[26] J. M. Otalora Goicochea,[2] P. Owen,[50] B. K. Pal,[53] A. Palano,[13,b] M. Palutan,[18] J. Panman,[35] A. Papanestis,[46] M. Pappagallo,[48] C. Parkes,[51] C. J. Parkinson,[50] G. Passaleva,[17] G. D. Patel,[49] M. Patel,[50] G. N. Patrick,[46] C. Patrignani,[19,i] C. Pavel-Nicorescu,[26] A. Pazos Alvarez,[34] A. Pellegrino,[38] G. Penso,[22,l] M. Pepe Altarelli,[35] S. Perazzini,[14,c] D. L. Perego,[20,j] E. Perez Trigo,[34] A. Pérez-Calero Yzquierdo,[33] P. Perret,[5] M. Perrin-Terrin,[6] G. Pessina,[20] K. Petridis,[50] A. Petrolini,[19,i] A. Phan,[53] E. Picatoste Olloqui,[33] B. Pie Valls,[33] B. Pietrzyk,[4] T. Pilař,[45] D. Pinci,[22] S. Playfer,[47] M. Plo Casasus,[34] F. Polci,[8] G. Polok,[23] A. Poluektov,[45,31] E. Polycarpo,[2] D. Popov,[10] B. Popovici,[26] C. Potterat,[33] A. Powell,[52] J. Prisciandaro,[36] V. Pugatch,[41] A. Puig Navarro,[36] W. Qian,[3] J. H. Rademacker,[43] B. Rakotomiaramanana,[36] M. S. Rangel,[2] I. Raniuk,[40] N. Rauschmayr,[35] G. Raven,[39] S. Redford,[52] M. M. Reid,[45] A. C. dos Reis,[1] S. Ricciardi,[46] A. Richards,[50] K. Rinnert,[49] V. Rives Molina,[33] D. A. Roa Romero,[5] P. Robbe,[7] E. Rodrigues,[48,51] P. Rodriguez Perez,[34] G. J. Rogers,[44] S. Roiser,[35] V. Romanovsky,[32] A. Romero Vidal,[34] J. Rouvinet,[36] T. Ruf,[35] H. Ruiz,[33] G. Sabatino,[21,k] J. J. Saborido Silva,[34] N. Sagidova,[27] P. Sail,[48] B. Saitta,[15,d] C. Salzmann,[37] B. Sanmartin Sedes,[34] M. Sannino,[19,i] R. Santacesaria,[22]

C. Santamarina Rios,[34] R. Santinelli,[35] E. Santovetti,[21,k] M. Sapunov,[6] A. Sarti,[18,l] C. Satriano,[22,m] A. Satta,[21] M. Savrie,[16,e] D. Savrina,[28] P. Schaack,[50] M. Schiller,[39] H. Schindler,[35] S. Schleich,[9] M. Schlupp,[9] M. Schmelling,[10] B. Schmidt,[35] O. Schneider,[36] A. Schopper,[35] M.-H. Schune,[7] R. Schwemmer,[35] B. Sciascia,[18] A. Sciubba,[18,l] M. Seco,[34] A. Semennikov,[28] K. Senderowska,[24] I. Sepp,[50] N. Serra,[37] J. Serrano,[6] P. Seyfert,[11] M. Shapkin,[32] I. Shapoval,[40,35] P. Shatalov,[28] Y. Shcheglov,[27] T. Shears,[49,35] L. Shekhtman,[31] O. Shevchenko,[40] V. Shevchenko,[28] A. Shires,[50] R. Silva Coutinho,[45] T. Skwarnicki,[53] N. A. Smith,[49] E. Smith,[52,46] M. Smith,[51] K. Sobczak,[5] F. J. P. Soler,[48] A. Solomin,[43] F. Soomro,[18,35] D. Souza,[43] B. Souza De Paula,[2] B. Spaan,[9] A. Sparkes,[47] P. Spradlin,[48] F. Stagni,[35] S. Stahl,[11] O. Steinkamp,[37] S. Stoica,[26] S. Stone,[53] B. Storaci,[38] M. Straticiuc,[26] U. Straumann,[37] V. K. Subbiah,[35] S. Swientek,[9] M. Szczekowski,[25] P. Szczypka,[36,35] T. Szumlak,[24] S. T'Jampens,[4] M. Teklishyn,[7] E. Teodorescu,[26] F. Teubert,[35] C. Thomas,[52] E. Thomas,[35] J. van Tilburg,[11] V. Tisserand,[4] M. Tobin,[37] S. Tolk,[39] S. Topp-Joergensen,[52] N. Torr,[52] E. Tournefier,[4,50] S. Tourneur,[36] M. T. Tran,[36] A. Tsaregorodtsev,[6] N. Tuning,[38] M. Ubeda Garcia,[35] A. Ukleja,[25] D. Urner,[51] U. Uwer,[11] V. Vagnoni,[14] G. Valenti,[14] R. Vazquez Gomez,[33] P. Vazquez Regueiro,[34] S. Vecchi,[16] J. J. Velthuis,[43] M. Veltri,[17,g] G. Veneziano,[36] M. Vesterinen,[35] B. Viaud,[7] I. Videau,[7] D. Vieira,[2] X. Vilasis-Cardona,[33,n] J. Visniakov,[34] A. Vollhardt,[37] D. Volyanskyy,[10] D. Voong,[43] A. Vorobyev,[27] V. Vorobyev,[31] H. Voss,[10] C. Voß,[55] R. Waldi,[55] R. Wallace,[12] S. Wandernoth,[11] J. Wang,[53] D. R. Ward,[44] N. K. Watson,[42] A. D. Webber,[51] D. Websdale,[50] M. Whitehead,[45] J. Wicht,[35] D. Wiedner,[11] L. Wiggers,[38] G. Wilkinson,[52] M. P. Williams,[45,46] M. Williams,[50,p] F. F. Wilson,[46] J. Wishahi,[9] M. Witek,[23,35] W. Witzeling,[35] S. A. Wotton,[44] S. Wright,[44] S. Wu,[3] K. Wyllie,[35] Y. Xie,[47] F. Xing,[52] Z. Xing,[53] Z. Yang,[3] R. Young,[47] X. Yuan,[3] O. Yushchenko,[32] M. Zangoli,[14] M. Zavertyaev,[10,a] F. Zhang,[3] L. Zhang,[53] W. C. Zhang,[12] Y. Zhang,[3] A. Zhelezov,[11] L. Zhong,[3] and A. Zvyagin[35]

(LHCb Collaboration)

[1]*Centro Brasileiro de Pesquisas Físicas (CBPF), Rio de Janeiro, Brazil*
[2]*Universidade Federal do Rio de Janeiro (UFRJ), Rio de Janeiro, Brazil*
[3]*Center for High Energy Physics, Tsinghua University, Beijing, China*
[4]*LAPP, Université de Savoie, CNRS/IN2P3, Annecy-Le-Vieux, France*
[5]*Clermont Université, Université Blaise Pascal, CNRS/IN2P3, LPC, Clermont-Ferrand, France*
[6]*CPPM, Aix-Marseille Université, CNRS/IN2P3, Marseille, France*
[7]*LAL, Université Paris-Sud, CNRS/IN2P3, Orsay, France*
[8]*LPNHE, Université Pierre et Marie Curie, Université Paris Diderot, CNRS/IN2P3, Paris, France*
[9]*Fakultät Physik, Technische Universität Dortmund, Dortmund, Germany*
[10]*Max-Planck-Institut für Kernphysik (MPIK), Heidelberg, Germany*
[11]*Physikalisches Institut, Ruprecht-Karls-Universität Heidelberg, Heidelberg, Germany*
[12]*School of Physics, University College Dublin, Dublin, Ireland*
[13]*Sezione INFN di Bari, Bari, Italy*
[14]*Sezione INFN di Bologna, Bologna, Italy*
[15]*Sezione INFN di Cagliari, Cagliari, Italy*
[16]*Sezione INFN di Ferrara, Ferrara, Italy*
[17]*Sezione INFN di Firenze, Firenze, Italy*
[18]*Laboratori Nazionali dell'INFN di Frascati, Frascati, Italy*
[19]*Sezione INFN di Genova, Genova, Italy*
[20]*Sezione INFN di Milano Bicocca, Milano, Italy*
[21]*Sezione INFN di Roma Tor Vergata, Roma, Italy*
[22]*Sezione INFN di Roma La Sapienza, Roma, Italy*
[23]*Henryk Niewodniczanski Institute of Nuclear Physics Polish Academy of Sciences, Kraków, Poland*
[24]*AGH University of Science and Technology, Kraków, Poland*
[25]*National Center for Nuclear Research (NCBJ), Warsaw, Poland*
[26]*Horia Hulubei National Institute of Physics and Nuclear Engineering, Bucharest-Magurele, Romania*
[27]*Petersburg Nuclear Physics Institute (PNPI), Gatchina, Russia*
[28]*Institute of Theoretical and Experimental Physics (ITEP), Moscow, Russia*
[29]*Institute of Nuclear Physics, Moscow State University (SINP MSU), Moscow, Russia*
[30]*Institute for Nuclear Research of the Russian Academy of Sciences (INR RAN), Moscow, Russia*
[31]*Budker Institute of Nuclear Physics (SB RAS) and Novosibirsk State University, Novosibirsk, Russia*
[32]*Institute for High Energy Physics (IHEP), Protvino, Russia*
[33]*Universitat de Barcelona, Barcelona, Spain*

[34]*Universidad de Santiago de Compostela, Santiago de Compostela, Spain*
[35]*European Organization for Nuclear Research (CERN), Geneva, Switzerland*
[36]*Ecole Polytechnique Fédérale de Lausanne (EPFL), Lausanne, Switzerland*
[37]*Physik-Institut, Universität Zürich, Zürich, Switzerland*
[38]*Nikhef National Institute for Subatomic Physics, Amsterdam, The Netherlands*
[39]*Nikhef National Institute for Subatomic Physics and VU University Amsterdam, Amsterdam, The Netherlands*
[40]*NSC Kharkiv Institute of Physics and Technology (NSC KIPT), Kharkiv, Ukraine*
[41]*Institute for Nuclear Research of the National Academy of Sciences (KINR), Kyiv, Ukraine*
[42]*University of Birmingham, Birmingham, United Kingdom*
[43]*H.H. Wills Physics Laboratory, University of Bristol, Bristol, United Kingdom*
[44]*Cavendish Laboratory, University of Cambridge, Cambridge, United Kingdom*
[45]*Department of Physics, University of Warwick, Coventry, United Kingdom*
[46]*STFC Rutherford Appleton Laboratory, Didcot, United Kingdom*
[47]*School of Physics and Astronomy, University of Edinburgh, Edinburgh, United Kingdom*
[48]*School of Physics and Astronomy, University of Glasgow, Glasgow, United Kingdom*
[49]*Oliver Lodge Laboratory, University of Liverpool, Liverpool, United Kingdom*
[50]*Imperial College London, London, United Kingdom*
[51]*School of Physics and Astronomy, University of Manchester, Manchester, United Kingdom*
[52]*Department of Physics, University of Oxford, Oxford, United Kingdom*
[53]*Syracuse University, Syracuse, New York, USA*
[54]*Pontifícia Universidade Católica do Rio de Janeiro (PUC-Rio), Rio de Janeiro, Brazil Universidade Federal do Rio de Janeiro (UFRJ), Rio de Janeiro, Brazil*
[55]*Institut für Physik, Universität Rostock, Rostock, Germany Physikalisches Institut, Ruprecht-Karls-Universität Heidelberg, Heidelberg, Germany*

[a]Also at LIFAELS, La Salle, Universitat Ramon Llull, Barcelona, Spain.
[b]Also at Università di Firenze, Firenze, Italy.
[c]Also at Università della Basilicata, Potenza, Italy.
[d]Also at Università di Modena e Reggio Emilia, Modena, Italy.
[e]Also at Università di Milano Bicocca, Milano, Italy.
[f]Also at Università di Bologna, Bologna, Italy.
[g]Also at Università di Roma Tor Vergata, Roma, Italy.
[h]Also at Università di Genova, Genova, Italy.
[i]Also at Università di Ferrara, Ferrara, Italy.
[j]Also at Università di Cagliari, Cagliari, Italy.
[k]Also at Hanoi University of Science, Hanoi, Viet Nam.
[l]Also at Università di Bari, Bari, Italy.
[m]Also at Università di Roma La Sapienza, Roma, Italy.
[n]Also at Università di Urbino, Urbino, Italy.
[o]Also at Massachusetts Institute of Technology, Cambridge, MA, USA.
[p]Also at P.N. Lebedev Physical Institute, Russian Academy of Science (LPI RAS), Moscow, Russia.